

# An Image Processing Approach to Characterizing Choroidal Blood Flow

G. J. Klein,\* R. H. Baumgartner,†‡ and R. W. Flower\*†

**Indocyanine green (ICG) dye angiography has made possible routine visualization of choroidal blood flow in the human eye; however, to date, its clinical utility has been limited. An overlying layer of densely pigmented tissue and the complex, multilayered vascular structure of the choroid combine to produce angiographic images of low contrast which are difficult to interpret. Conventional image processing can enhance individual images of the blood vessels, but this approach contributes no information about the dynamics of blood flow. Using relatively inexpensive, commercially available personal computer hardware, angiographic image processing algorithms were developed which appear to characterize uniquely a subject choroid in terms of various blood flow parameters. We believe this to be the first successfully demonstrated approach to routinely characterizing the human choroidal circulation in a way that conserves spatial distribution of blood flow dynamics across the entire observed choroidal area. The computer system allows acquisition of digital images from photographic film negatives; alternatively, real-time direct digitization of images from a high-resolution video camera is possible. Once acquired, the digitized data are manipulated according to various algorithms that employ time-sequence analysis to generate two-dimensional curves or three-dimensional surfaces which characterize the choroidal circulation. The unique correspondence of each three-dimensional surface to the subject choroidal circulation from which it was derived is demonstrated. Grouping the characteristic three-dimensional surfaces according to various topographic features in common may provide a basis for discriminating between normal and abnormal choroidal circulations. Invest Ophthalmol Vis Sci 31:629-637, 1990**

The importance of choroidal blood flow to maintenance of the sensory retina—especially the fovea—has long been recognized; however, its role in the etiology of retinal diseases is not well understood. In large part this has resulted from inability to visualize routinely the choroidal vasculature and to differentiate between normal and abnormal blood flow through it.

Fluorescein angiography of the choroidal vasculature is hampered by the presence of macular xanthophyll, retinal pigment epithelium, and choroidal pigment—all of which block the visible light wavelengths absorbed and emitted by the dye—and by the rapid extravasation of unbound fluorescein molecules which stain choroidal tissue. Although indocyanine green (ICG) dye angiography permits visual-

ization of the choroidal vasculatures by avoiding the shortcomings of fluorescein associated with its spectral and blood binding characteristics,<sup>1</sup> the thick, multilayered structure of the choroidal vasculature and the greater blood velocity through it (compared to retinal blood velocity) present difficulties related to interpreting choroidal angiographic studies. The rapidly changing choroidal dye filling patterns do not readily lend themselves to the same by-eye-only evaluation used to interpret retinal fluorescein angiograms; apparently, a much more sophisticated approach than visual pattern recognition is required. If the clinical potential of ICG choroidal angiography is to be fully realized, a method for recognizing and classifying choroidal dye filling patterns must be developed by which clinically significant differences between normal and abnormal choroidal circulations can be routinely distinguished.

To address the problem of choroidal angiogram interpretation, we have developed a personal-computer-based image analysis system and software. We consider two aspects of our approach particularly noteworthy: first, since experience has shown that solutions to problems based on expensive or custom-made instrumentation do not readily find acceptance in the clinical environment, only relatively inexpen-

From the \*Johns Hopkins University Applied Physics Laboratory, Laurel, Maryland; the †Wilmer Ophthalmological Institute, Baltimore, Maryland; and the ‡St. Gallen Eye Clinic, St. Gallen, Switzerland.

Supported in part by the U. S. Navy under Contract N00039-87-C-5301 and by a grant from Switzerland's Nationalfonds.

Submitted for publication: February 20, 1989; accepted August 7, 1989.

Reprint requests: Robert W. Flower, The Johns Hopkins University Applied Physics Laboratory, Johns Hopkins Road, Laurel, MD 20707.

sive, commercially available hardware components were used. Second, most of the previous image processing efforts related to ocular angiography—including our own—have concentrated on enhancement of static images, but since blood flow is a dynamic process, our software algorithm development focused on time-sequence analysis of angiograms.

The computer system is used to acquire digitally a sequence of angiographic images. From that database, a three-dimensional surface is generated, the  $x$ - $y$  plane of which corresponds to the fundus area in the angiograms and the topography of which represents the dye-filling dynamics of the area. The computer system and software algorithms are described below, and the correspondence of each three-dimensional surface to the subject choroidal circulation from which it was generated is demonstrated. It appears that similarities and differences between these three-dimensional surfaces may constitute a basis upon which high-speed choroidal angiographic studies can be classified and normal versus abnormal circulation patterns can be distinguished. We believe this to be the first demonstrated approach to routinely characterizing the human choroidal circulation in a way that conserves spatial distribution of blood flow dynamics across the entire observed choroidal area.

### Materials and Methods

#### Subjects

Data for this investigation were obtained from ICG angiograms made of human subjects and digitally recorded at 15 images/sec. In each case, 0.5 ml of 25 mg/ml ICG dye (Cardio-Green; Becton Dickinson Microbiology, Hunt Valley, MD) in aqueous solvent was injected into an anti-cubital vein, followed immediately by a 5-ml saline flush. Details of the modified Zeiss (Oberkochen, West Germany) fundus camera used to record the angiograms are described elsewhere.<sup>2</sup> A 30° field of the posterior choroid, centered approximately on the fovea, was observed in each subject.

Because only one angiographic study was available from each human subject, serial angiographic studies were made of several adult rhesus monkeys so that choroidal dye filling data obtained at different times from the same subject could be compared. The monkeys were intubated and kept lightly anesthetized with fluothane. ICG dye was injected into the saphenous vein as a 0.25 ml bolus of 12 mg/ml dye in aqueous solvent, followed immediately by a 3-ml saline flush. In several instances, however, different injected dye bolus concentrations were used for the se-

rial studies in order to provide comparison of the effects of producing a different maximum dye fluorescence during each angiographic study.

The use of animals in this investigation conformed to the ARVO Resolution on the Use of Animals in Research. Informed consent was obtained from all human subjects prior to the study.

#### Digitization of Angiogram Images

Digitization of angiographic data is achieved by acquiring real-time images from the fundus camera with a high-resolution video camera (thermoelectrically cooled CCD camera model CCD 5000; Fairchild Weston Systems, Milipitas, CA) connected to a frame grabber (DT-2861; Data Translation, Marlboro, MA) which translated them into 480 × 512 pixel × 256 gray-level, or brightness, arrays. One pixel in this array corresponds to approximately a 13- $\mu$ m spot on the retina. Once an angiographic sequence is digitally acquired, the sequence is preprocessed to align the images with each other and to remove noise introduced by the video camera. Alignment of successive angiographic images is carried out by manually panning and scrolling an image in software while a reference image is alternately displayed. In this manner, alignment to within a few pixels is easily attained. For greater accuracy, an auxiliary program can be invoked which uses Fourier phase techniques<sup>3</sup> and performs final alignment without manual inputs. The net result of the digitization process is a sequence of aligned images which may be stored on an optical disk.

#### Time-Sequence Analysis

The computer system allows a digitized image to be divided into a grid pattern of segments defined by any number of horizontal and vertical divisions such that the total number of segments is less than 1024. Thus, the segment size can be made small enough that individual anatomic choroidal structures, such as the lobules of the choriocapillaris, are isolated. In the process of analyzing an angiographic study, as each digitized image is recalled from storage, it is divided into segments, and the average gray level, or brightness, for each segment is recorded into a data array. Averaging is used in order to transform the data to a more rapidly manageable format.

As images are analyzed, processed data are stored on a hard disk. Once average gray-level data for an entire angiographic sequence have been recorded, various characteristic dye-filling dynamics can be determined by analyzing the relative brightness changes in any fundus region of interest. These characteris-

tics, indicative of choroidal blood flow dynamics, can be represented as two- and three-dimensional plots.

### Data Analysis and Display Algorithms

Analysis of recorded average gray level data is based upon the following model. Each segment into which the choroid is divided defines a separate elastic compartment having one or more inlets (arterioles) and one or more outlets (venules). The volume of a compartment is considered to be the aggregate volume of all of the vessels and vessel segments contained in a full-thickness plug of choroidal tissue, bounded by the projections of the four lines that define the sides of the sector; compartment volume does not include intervascular spaces and may vary with the cardiac cycle.

At any given time, each choroidal compartment underlying each segment is associated with a mean dye concentration and hence with a total level of dye fluorescence as well. Assuming that maximum dye concentration remains below that at which fluorescence quenching occurs,<sup>4</sup> during the dye-filling phase the total fluorescence from any particular choroidal segment will be a monotonically increasing function of the total amount of dye within the compartment underlying that segment. That is, the resulting fluorescence of a given segment is the equal superposition of all vessels, regardless of depth from the retina. In addition, it is assumed that the ICG dye is uniformly mixed with blood by the time it reaches the eye; that the wavefront of dye-tagged blood entering the ocular vasculatures is well defined; that the bolus of dye-tagged blood remains integral during its passage through the choroidal vasculature; and that the volume of the dye-tagged blood bolus is greater than that of the observed choroidal vasculature.

Dye fluorescence is attenuated somewhat by pigment in choroidal tissue, by the pigment epithelium, and to a lesser extent, by the overlying retina. The attenuation for a given region of the fundus is assumed to be a multiplicative constant, and its effect upon spatially varying brightness levels is assumed to be negligible compared to brightness variations due to varying dye concentrations. This assumption is reasonable in view of the uniformity with which the non-dye-filled fundus reflects 800-nm light.<sup>5</sup>

With the above assumptions, if observations are begun just before the appearance of dye anywhere in the choroid, then the fluorescent brightness of a given sector can be used as a relative measure of the total blood volume which has progressed through that sector at any given time. In order to relate average time-

varying relative changes in gray level to various choroidal blood flow characteristics, the following parameters and algorithms are used:

*Time-varying average grey level:* Figure 1 shows an idealized characterization of the average time-varying gray level for a single sector of a choroid. This plot indicates that the average gray level remains at some background level,  $I_0$ , until the first appearance of dye occurs at time  $t_0$ . Once dye enters the compartment under this sector, the average gray level increases to a maximum level,  $I_{max}$ , at time  $t_{max}$  when the compartment is completely filled with dye.  $I_1$ ,  $I_2$ ,  $t_1$ , and  $t_2$  indicate arbitrary intermediate gray levels and the times at which they occur.

*Instantaneous dye filling rate:* Since the average gray level of a sector is a time-varying function,  $I = f(t)$ , the instantaneous filling rate of a sector is the first derivative of that function,  $\frac{dI}{dt} = \frac{df(t)}{dt}$ . In terms

of the model, changes in this rate are induced by blood pressure gradients and by changes in the dye concentration.

*Average dye-filling rate:* The average filling rate of a sector is defined by the ratio  $(I_2 - I_1)/(t_2 - t_1)$ . The data time interval,  $\Delta t$ , is defined as  $\Delta t = t_2 - t_1$ .  $\Delta t$  can be any interval during the angiogram; however, its length must be some integer multiple of the time between two successive images of the angiogram, up to  $\Delta t_{max} = t_{max} - t_0$ . Computed and displayed for

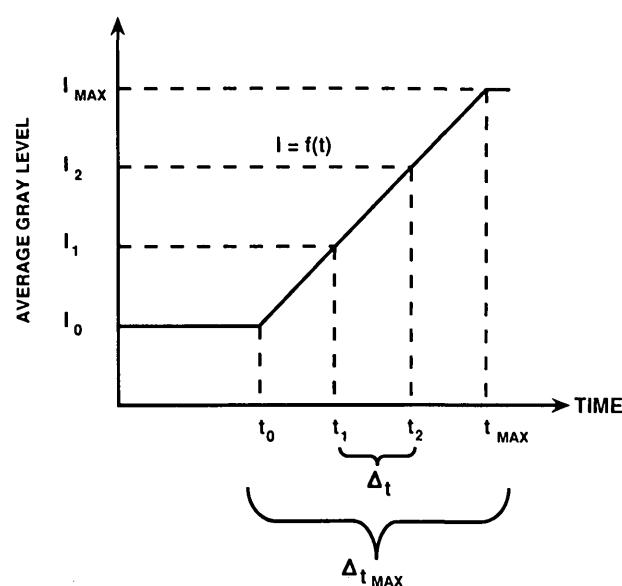


Fig. 1. Idealized time-varying average gray level of a single choroidal sector as ICG dye fills the vasculature beneath it. Dye first enters the segment at time  $t_0$ , corresponding to average sector brightness, or gray level,  $I_0$ .  $t_{max}$  is the time at which maximum dye fluorescence brightness,  $I_{max}$ , occurs.  $t_1$  and  $t_2$  are arbitrary intermediate times.

each sector, the relationships between average filling rates should make possible identification of areas of relative differences in choroidal blood flow.

In order to facilitate comparisons of various parameters computed for each of the sectors comprising the entire observed fundus area, it is convenient to visualize those parameters in terms of three-dimensional surfaces projected above the fundus area. Any blood flow parameter can be represented for each sector as a vector normal to the plane of the choroid, having its origin at the sector's center. Point-to-point connection of each vector end to all neighboring vector ends approximates a three-dimensional surface representing that particular choroidal blood flow parameter for the entire observed fundus area. For example, if the parameter of interest were the average dye-filling rate, then the elevated portion of the three-dimensional surface would correspond to a choroidal area of rapid dye filling and a lower portion to an area of less rapid filling. Once defined, a three-dimensional surface can easily be rotated in space about any axis for inspection or for comparison to other such surfaces. Also, the amplitude of the vectors defining the surface can be changed freely to facilitate these comparisons since only their relative magnitudes with respect to each other are of interest. The model and algorithms are such that determination of quantitative blood flow parameters for inter-subject comparisons is not possible. Nevertheless, the computer-generated topographies resulting from appropriately defined parameters should serve as a basis for distinguishing between normal and abnormal choroidal dye-filling patterns.

## Results

### Determination of the Ideal Segment Size

The three-dimensional surface-generation algorithm requires segmentation of the choroid. The greater the number of segments used, the greater the resolution of data displayed, but the time required to manipulate the data and perform necessary calculations becomes greater also. In order to find a reasonable balance between segment size and processing time, a series of three-dimensional surfaces characterizing average dye-filling rate were generated from the same digitized angiographic data set by using different choroidal segment areas of decreasing size. A series of such surfaces was generated for each of several representative angiogram sequences; one series is shown in Figure 2.

Segment areas smaller than those in a  $10 \times 15$  array did not produce significant refinements of the

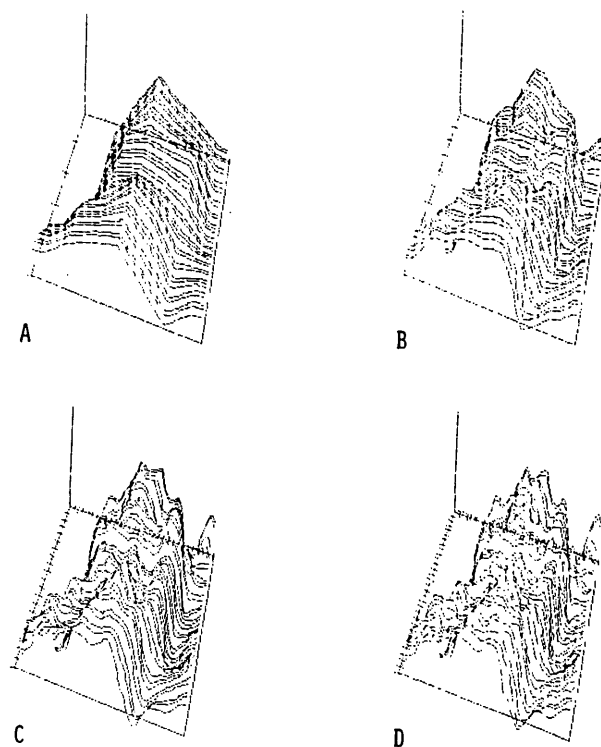
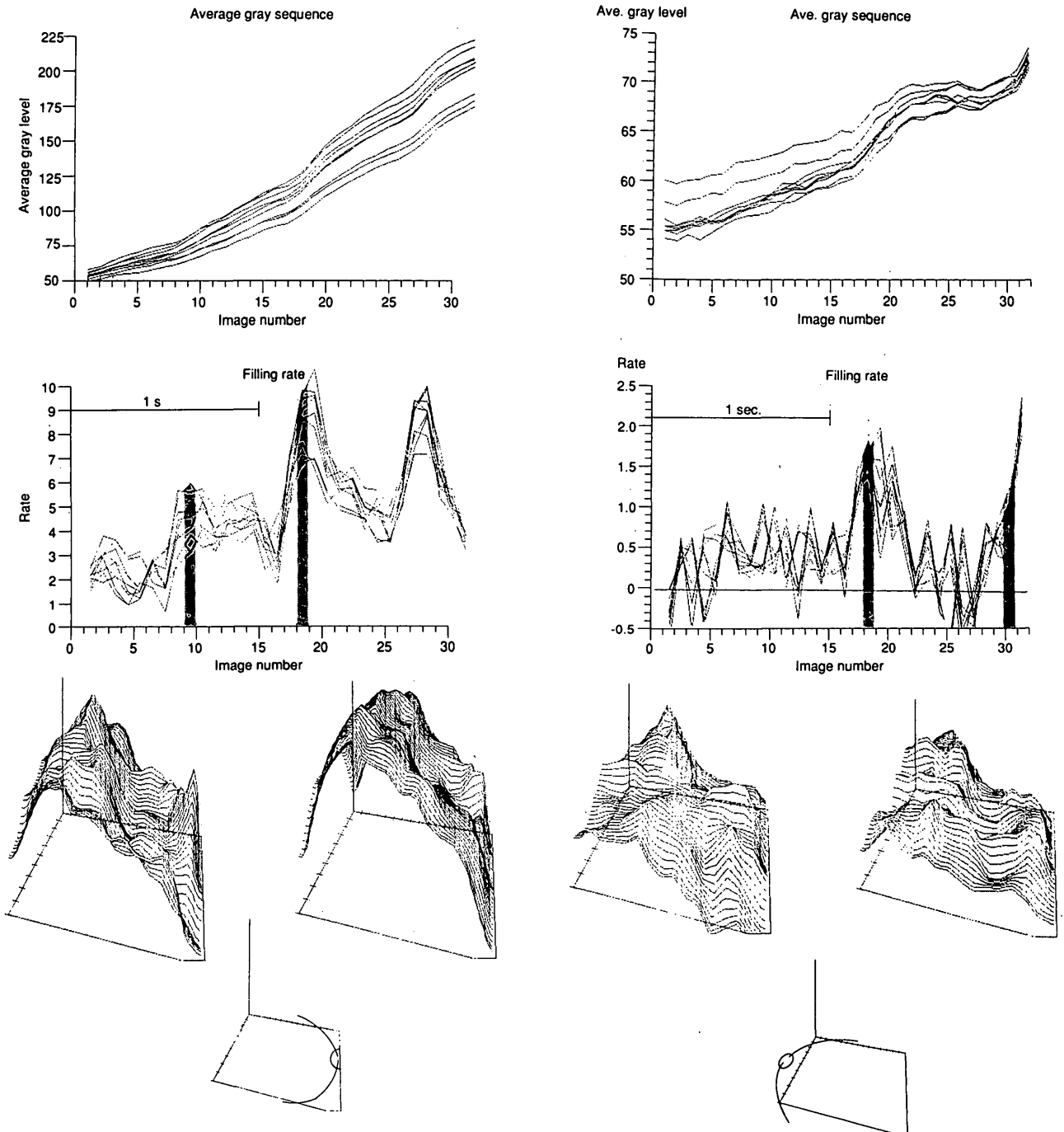


Fig. 2. Effect of sector size on the three-dimensional surface topography. Using the same digitized angiographic data set, average dye filling rates were computed using a sequence of different segment sizes, and the corresponding three-dimensional surfaces were generated. (A)  $5 \times 7$ -segment array. (B)  $10 \times 15$ -segment array. (C)  $20 \times 30$ -segment array. (D)  $30 \times 50$ -segment array.

major features in the three-dimensional surface characterizing each angiogram sequence; the higher-frequency information produced by using the smaller segments appeared to represent only noise and low-amplitude fine structure, which were viewed as unimportant for this investigation. Conversely, segment areas greater than those in a  $10 \times 15$  array produced surfaces devoid of significant features. It is notable that the  $10 \times 15$  array segment area (about  $0.25 \text{ mm}^2$ ) corresponds approximately to the area of the choriocapillaris lobules.<sup>6</sup> For the examples reported below,  $10 \times 15$  and  $10 \times 16$  segment arrays were used.

### Cyclic Pattern in Choroidal Dye Filling

Figures 3 and 4 demonstrate application of the instantaneous dye-filling rate and data-display algorithms using ICG angiograms from two human subjects. The top graph in each figure shows the time-varying average gray level for a number of individual choroidal segments clustered about the macula; at the bottom of each figure, the  $10 \times 16$  grid patterns overlying schematic representations of the fundus of each



**Fig. 3.** (left), 4 (right). Interim results used in generation of characteristic three-dimensional surfaces for each of two human choroidal angiogram sequences. For each subject, a schematic fundus representation at the bottom provides orientation by indicating location of the optic disc, fovea, and segmentation of the choroid used in application of the algorithm. *Top graphs:* The changing average brightness of nine clustered choroidal segments as they filled with ICG dye. These curves, which describe the time-varying average gray level of the choroidal segments, generally are monotonically increasing functions. *Center graphs:* The first derivatives of the curves in the top graphs. These represent the instantaneous rate of ICG dye filling of each choroidal segment as a function of time. Note the cyclic variation of filling rates; these are synchronous with the cyclic variations in heart rate, and hence, also with ocular blood pressure pulse. The shaded areas indicate the systolic periods; these are the periods for which choroidal segment filling rates are represented by the three-dimensional surfaces, below. *Three-dimensional surfaces:* For each entire choroidal area shown in the schematic fundus, filling rates which occur during each systolic period are represented by three-dimensional surfaces. The Z-axes are the magnitudes of the filling rates during systole. Note there is similarity between all surfaces from the same choroidal angiographic sequence, yet there are distinct differences between those from different choroids.

subject are depicted. The second graph, at center, shows the instantaneous dye filling rate obtained by taking the first derivative of the curves in the top graph.

In most subjects, as in these two examples, a cyclic variation was apparent in the instantaneous filling rate curves. The frequency of this variation was on the order of once per sec, approximately the frequency of each subject's cardiac cycle; the most rapidly increasing portion of each cycle presumably corresponds to the systolic phase of the subject's cardiac cycle. In those cases where  $\Delta t$  values could be defined to coincide with the systolic periods of the ocular pulse, the average filling rate during each systole was computed for all the choroidal sectors using the digitized gray level data from the corresponding angiogram images ( $\Delta t =$  two images, the shaded areas under the curves in Figures 4 and 5), and then from those results, a three-dimensional surface was gener-

ated to represent the distribution of average filling rates across the entire choroidal area during each systole.

### Three-Dimensional Surfaces Characterizing Choroidal Blood Flow

As demonstrated in Figures 3 and 4, the topographies of the surfaces generated from each human subject are quite similar to each other; yet there are notable differences between the topographies of surfaces from different subjects. Moreover, these topographies appear to be stable from day to day as demonstrated by the pairs of surfaces in Figure 5, which were generated from angiograms made from the same anesthetized monkey on different days; this stability was evident in the several monkeys we examined. These results indicate that a three-dimensional representation of average systolic filling rate may uniquely

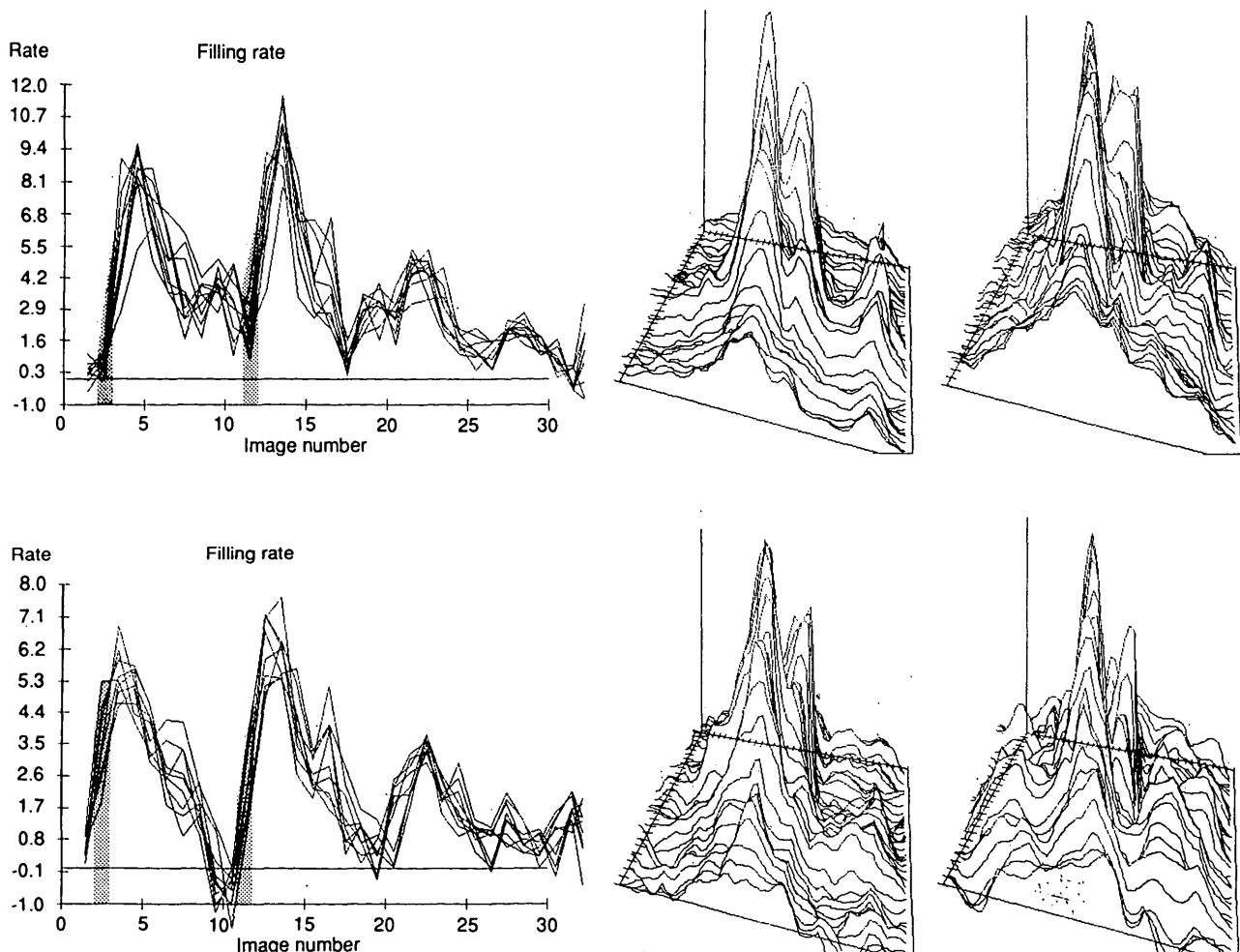


Fig. 5. Two three-dimensional surfaces generated from each of two angiographic sequences made of the same anesthetized monkey on different days. The filling rate curves to the left of each pair of surfaces show the ocular pulse pressures, and the shaded areas under these curves indicate the systolic time intervals ( $\Delta t$ ) used to compute the instantaneous filling rates used to generate each surface.

characterize the particular choroidal circulation from which it is derived. A second set of surfaces was generated for each of the subjects by defining  $\Delta t$  values corresponding to the diastolic periods; however, even though the topographies of these surfaces also were similar to each other, they were not similar to the degree of the systolic topographies.

Within a sequence of three-dimensional surfaces generated by incrementally moving a short  $\Delta t$  along the abscissa of the curve defining instantaneous filling rate, there was great dissimilarity between the topographies of any adjacent pair of surfaces. Moreover, there was a degree of variability among the surfaces generated from systoles occurring within such a sequence whenever the  $\Delta t$  happened to fall even slightly out of phase with the systolic periods. We did find, however, that adjacent pairs of the three-dimensional surfaces generated by moving a much larger  $\Delta t$  (large enough to encompass an entire cardiac cycle) along the abscissa bore greater similarities to each other, although fine topographic detail diminished.

Because of the 15 image/sec rate at which the angiograms were recorded, the likelihood of being able to define  $\Delta t$  values which coincide precisely with the systoles in any given angiographic study was small. To obviate this problem, three-dimensional surfaces were generated from average filling rates, which were computed for each choroidal segment using  $\Delta t_{\max}$ . Of

course,  $\Delta t_{\max}$  could not be the same for all the segments, since dye arrives at different segments at different times and then fills them at different rates. These surfaces also proved to be distinctive of the choroidal circulations from which they were derived. For example, the same three-dimensional surface topography could be generated from successive angiographic studies made of the same subject, even when changes were intentionally induced in the maximum fluorescence brightness produced during each study (see Figure 6).

## Discussion

As indicated earlier, the values of the attenuation factor for dye fluorescence and vascular volume used in the data analysis model are currently unknown; other factors not considered in this model also may affect the observed data. Quantitative measurements of choroidal blood flow parameters cannot be made; consequently, inferences made about choroidal blood flow from this investigation must be viewed for now as somewhat speculative. Nevertheless, the parameters considered in this study are valuable because they allow integration of information from an entire angiographic sequence into one representative diagram, the characteristic three-dimensional surface. Despite

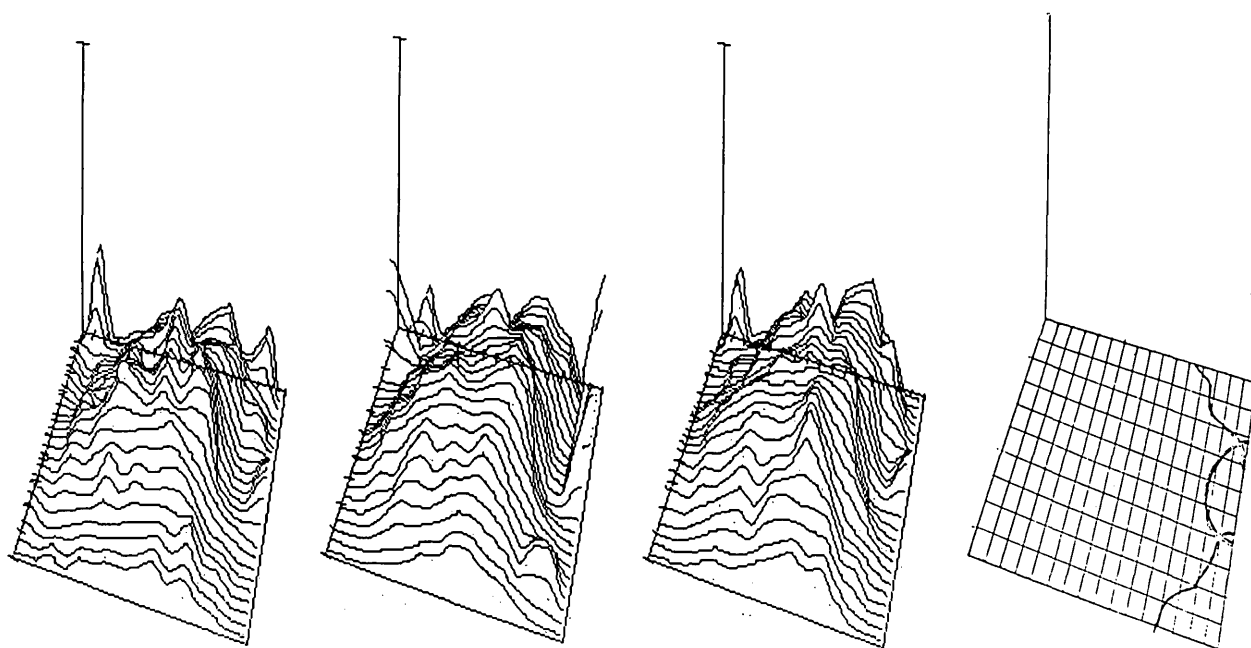


Fig. 6. Three three-dimensional surfaces generated from average choroidal dye-filling rates of an anesthetized monkey computed by using  $\Delta t_{\max}$  for each segment shown in the grid pattern of the schematic fundus on the right. Each surface was derived from a different set of angiographic data; the same dye bolus volume was injected each time, but the ICG dye concentration was varied in each case. The left surface represents a concentration of 6 mg/ml; the middle, 12 mg/ml; and the right, 24 mg/ml.

any speculative aspects of the model we used, the results demonstrated that it is possible by our methods to characterize different aspects of circulation dynamics of a subject choroid on the basis of ICG angiography. These characterizations facilitate comparisons between different sectors of the same subject choroid as well as between choroids of different subjects; no such comparisons could be made by simply viewing sequences of raw angiographic images.

A number of data analysis algorithms were considered during the course of this investigation, and most of them involved calculation of some form of the dye-filling rate, since it was apparent that each choroidal circulation contains a distinctive spatial distribution of filling rates. However, creation of an algorithm to detect and represent consistently each unique distribution was not straightforward. For example, choice of the particular time interval during an angiographic study to use in calculating filling rates was not clear; it was not until the cardiac-generated cyclic patterns were observed in plots of instantaneous dye-filling rates that it became feasible to define a time interval common to all choroidal circulations as a basis for generating three-dimensional surfaces individually representative of each circulation.

Since apparently a choroidal circulation can be characterized equally well from data obtained during any systolic period occurring during an angiographic sequence, the usual concern about recording the *initial* entry of dye into the vasculature essentially can be ignored. On the other hand, the need to identify clear cyclic patterns or to define data collection intervals ( $\Delta t$ ) precisely in phase with and of identical length to systolic periods, underscores the necessity of achieving adequate temporal resolution when recording choroidal angiograms.

Data intervals ( $\Delta t$  values) for calculation of average filling rates are comprised of two or more whole time-interval quanta whose lengths are dictated by the frame rate at which the angiograms were made. It is by chance that in some cases two or more data intervals can be defined to coincide almost precisely with systolic periods. Close examination of Figures 3 and 4 indicates that in these cases, all data intervals did not precisely correspond to the cardiac-generated cyclic patterns. If limited temporal resolution of angiogram sequences becomes a problem, in lieu of systole-generated three-dimensional surfaces, surfaces can be generated from average dye-filling rates computed from data throughout the dye-filling period,  $\Delta t_{\max}$ . Although the topographies of these surfaces apparently lack the degree of detailed information

about circulation dynamics contained in the systole-generated surfaces, they appear adequate to characterize uniquely the choroidal circulation (Fig. 5).

Although the surfaces generated during successive systolic periods of the ocular pulse pressure are not identical, they are quite similar in terms of their spatial distributions of major deviations and depressions. Close examination of the pairs of surfaces in Figures 3 and 4 shows that the locations of areas of high dye-filling rates relative to those of low filling rates remain stable from ocular pulse to ocular pulse for each subject, even though actual surface elevation above specific points on the fundus reference plane can vary from pulse to pulse. This finding is not surprising, considering that blood can enter the complex choroidal vascular network from more than 20 feeding arterioles and the actual flow rate through each depends on the instantaneous relationships between pressure differentials and vascular resistances throughout the network. Apparently, those relationships normally vary within a fairly narrow range, accounting for the pulse-to-pulse variations seen in the characteristic three-dimensional surface of a given subject, as demonstrated in Figures 3 and 4; that narrow range appears to remain stable from day to day, as demonstrated in Figure 5.

Variations in choroidal anatomy from subject to subject, however, would be expected to produce different sets of pressure-differential and vascular resistances for each subject, resulting in uniquely different characteristic three-dimensional surfaces for each. However, just as all normal eyes, despite individual variations, contain the same major choroidal vascular anatomical features, the characteristic three-dimensional surfaces of normal eyes can be expected to contain similar major features. For example, the prominent "mountain ranges" in the surfaces in Figures 3 and 4 overlie the points of insertion of the short posterior ciliary arteries, places where the highest choroidal dye filling rates would be expected.

Grouping the characteristic three-dimensional surfaces according to various topographic features they have in common can provide, for the first time, a basis for discriminating between normal and abnormal choroidal circulations, and do so in a way that conserves the spatial distribution of blood flow dynamics across the entire choroidal area observed.<sup>7</sup> This approach differs from others, such as that of Prunte and Niesel,<sup>8</sup> which characterize a large choroidal area in terms of a single numeric value. The advantage to our approach is that suspicious regions in a topography can be correlated directly to specific areas of the choroid. Ultimately, this ability to characterize individual choroidal circulations may make it possi-



ble to relate subtle changes in choroidal blood flow to various ocular pathologies.

**Key words:** choroidal angiography, indocyanine green (ICG) dye angiography, image analysis, choroidal blood flow dynamics, hemodynamics

### Acknowledgment

The authors gratefully acknowledge the support they received from Becton Dickinson Microbiology Systems, Hunt Valley, Maryland, who supplied the ICG dye (Cardio-Green) used in these studies.

### References

1. Flower RW and Hochheimer BF: A clinical technique and apparatus for simultaneous angiography of the separate retinal and choroidal circulations. *Invest Ophthalmol* 12:248, 1973.
2. Bischoff P and Flower RW: Ten years experience with choroidal angiography using indocyanine green dye: A new routine examination or an epilogue? *Doc Ophthalmol* 60:235, 1985.
3. De Castro E, Cristini G, Martelli A, Morandi C, and Vascotto M: Compensation of random eye motion in television ophthalmoscopy: Preliminary results. *IEEE Transactions on Medical Imaging* MI-6(1):74, 1987.
4. Flower RW and Hochheimer BF: Quantification of indicator dye concentration in ocular blood vessels. *Exp Eye Res* 25:103, 1977.
5. Flower RW: Infra-red absorption angiography of the choroid and some observations on the effects of high intra-ocular pressures. *Am J Ophthalmol* 74:600, 1972.
6. Hunold W: Personal communication.
7. Flower RW, Klein GJ, Fryczkowski AW, and Baumgartner RH: Observations on the choroidal circulations of normal and diabetic monkeys using ICG dye fluorescence angiography. Publication pending.
8. Prunte C and Niesel P: Quantification of choroidal blood-flow parameters using indocyanine green video-fluorescence angiography and statistical picture analysis. *Graefes Arch Clin Exp Ophthalmol* 226:55, 1988.